Medium effects on intermediate-energy one-nucleon removal cross sections

F. Flavigny and A. Obertelli
CEA, Centre de Saclay, IRFU/Service de Physique Nucléaire, F-91191 Gif-sur-Yvette, France

I. Vidaña
CFC, Departamento de Física, Universidade de Coimbra, P-3004-516 Coimbra, Portugal

(Received 27 April 2009; published 26 June 2009)

The influence of Pauli-blocking medium effects on intermediate-energy one-nucleon removal cross sections for sd-shell nuclei have been investigated using density-dependent nucleon-nucleon interaction cross sections within the S-matrix formalism under the Glauber approximation. All considered prescriptions for the density dependence result in a reduction of the one-nucleon removal cross sections. The effect is smaller than 20% for incident energies between 50 and 100 MeV/nucleon, and smaller than a few percent above 200 MeV/nucleon.

DOI: 10.1103/PhysRevC.79.064617 PACS number(s): 21.10.Jx, 24.10.−i, 24.50.+g, 25.60.Dz

I. INTRODUCTION

Direct nuclear reactions, collisions during which very few nuclear degrees of freedom are modified, are commonly used to access information on nucleonic shell occupancies through the extraction of spectroscopic factors S_f. Spectroscopic factors are defined as the overlap between populated final states and the initial state of the wave function [1]. In the case of single-orbit nucleon stripping reactions, they are determined as the ratio of the measured cross section $\sigma_{\rm exp}$ to the theoretical single-particle cross section $\sigma_{\rm sp}$, $S_f \propto \sigma_{\rm exp}/\sigma_{\rm sp}$, assuming the reaction mechanism is correctly modeled. Several stripping processes have been used to study ground-state properties across the nuclear chart. Proton shell structure has been largely studied via $(e, e' p)$ knockout reactions on stable nuclei [2]. Shell structure of unstable nuclei can be investigated in inverse kinematics by low-energy transfer reactions analyzed within the distorted wave Born approximation (DWBA) or coupled-channel formalisms [3] and by intermediate-energy nucleon-removal reactions usually analyzed within the Glauber approximation [4]. These reactions have been shown to provide rather consistent spectroscopic factors for stable or exotic nuclei [5–7]. The question is still open regarding the stripping of deeply-bound nucleons in very asymmetric systems [8]. In any case, uncertainties on the reaction mechanism impacts directly the reliability of calculated single-particle cross sections, limiting our capability to extract absolute spectroscopic factors.

Among the above mentioned experimental probes, intermediate-energy nucleon removal reactions are a unique and robust tool to perform the spectroscopy of very exotic nuclei that are produced at intensities as small as a few particles per second [9]. These reactions have been extensively used to study very asymmetric systems displaying a large excess or a deficiency of neutrons compared to stable isotopes. Single-particle cross sections for such reactions can be evaluated using the Glauber approximation. Such an approximation, formulated within the S-matrix theory, is valid when the intrinsic nucleon velocity is negligible compared to the projectile-target relative velocity. It is considered fulfilled for energies above $\sim$30 MeV/nucleon [9]. Microscopic S-matrix calculations rely essentially on two types of input: (i) nuclear densities (target, projectile, and single-particle wave functions) and (ii) the in-medium nucleon-nucleon (NN) cross sections [10,11] or a nucleon-nucleon, or nucleon-target, optical potential to account for the stripping process [12]. The effect of the kind of densities considered in S-matrix calculations on knockout cross sections has been discussed for sd-shell nuclei [13]. When densities from Skyrme energy density functional (EDF) calculations are used, the final one-nucleon knockout cross section may vary up to several percents depending on the parametrization used. Moreover, deformation can modify the single-particle cross sections by up to 30% for well deformed systems [14,15].

The NN interaction to consider in the calculation is expected to be modified in the nuclear medium compared to the free case due to Pauli-blocking which partially reduces the phase space of collisions, and due to the modification of the single-particle properties of the nucleon at finite density. Indeed, several authors have studied the in-medium NN scattering problem using different approaches. There exists in the literature calculations of the in-medium NN cross sections based on the nonrelativistic Brueckner theory [16–22] as well as its relativistic version, the Dirac-Brueckner theory [23–26], or the variational method [27]. These medium effects can be taken into account via a density dependence (DD) of the NN interaction cross sections or of the effective nucleon-nucleon optical potential. However, they are often disregarded in the calculation of one-nucleon removal cross sections where mainly free-space NN cross sections are considered. In the specific case of two-neutron halo removal cross sections at intermediate energies and total reaction cross sections on light neutron-rich nuclei, their effect has already been studied and shown to be small [28].

Using in-medium NN cross sections based on a Brueckner calculation [22] and on two different parametrizations by Li and Machleidt [24,25], and by Xiangzhou *et al.* [29], we study in this paper the effect of the in-medium NN interaction on one-nucleon removal reactions at intermediate energies on sd-shell nuclei and evaluate its impact on single-particle cross sections.

 ©2009 The American Physical Society

II. FORMALISM

A. *S*-matrix formalism

In order to implement density-dependent effective NN interaction cross sections in the S-matrix formalism, we have developed a dedicated code that calculates one-nucleon removal cross sections within the Glauber approximation. Similar developments have been performed to investigate the effect of density dependence on reaction cross sections [28]. In the following, we assume inverse-kinematics reactions. The one-nucleon removal cross section is calculated using the eikonal formalism [10,30] and consists of a stripping and a diffractive part, i.e., $\sigma = \sigma_{\rm str} + \sigma_{\rm diff}$. The projectile wave function $|\psi\rangle$ is defined as a core wave function $|\phi_C\rangle$ complemented with the wave function of the removed nucleon $|\phi_N\rangle$. Calculations are based on two main quantities: the elastic S matrices for the core (S_C) and the removed nucleon (S_N). In an impact-parameter representation, the stripping part of the cross section is calculated as

$$\sigma_{\rm str} = 2\pi \int bdb \int d\vec{r}\, |\phi_N(\vec{r})|^2 |S_C(\vec{b}_C)|^2 (1 - |S_N(\vec{b}_N)|^2), \tag{1}$$

where $\vec{b}_C, \vec{b}_N$ are the impact parameters of the core and of the removed nucleon, respectively. The elastic S matrix for the core-target system S_C is defined from the target (T) and core densities as well as from the in-medium NN cross sections $\sigma_{NN}(E, \rho)$ that depends on both the incident energy and the total density of the system, i.e., the sum of projectile and target densities $\rho = \rho_P + \rho_T$. At an impact parameter $\vec{b}$, the S matrix is defined as a phase shift $S_C(\vec{b}) = \exp(i\,\chi_C(\vec{b}))$ with a complex phase

$$\chi_C(\vec{b}) = -\int dz \int d\vec{r'}\, \sigma_{NN}(E, \rho(\vec{r'}))\, \rho_C(\vec{r'})\, \rho_T(|\vec{b} - \vec{r'}|), \tag{2}$$

where the density ρ is taken at point $\vec{r'}$ and the trajectory of the center of mass is considered as a straight line along the z axis. We explicitly differentiate $T_z = 0$ and $T_z = 1$ interactions by considering proton and neutron densities separately. The diffractive part is obtained from the same S matrices as

$$\sigma_{\rm diff} = 2\pi \int bdb \left\{ \int d\vec{r}\, |\phi_N(\vec{r})|^2\, |(1 - S_C(\vec{b}_C) S_N(\vec{b}_N))|^2 - \left| \int d\vec{r}\, |\phi_N(\vec{r})|^2 (1 - S_C(\vec{b}_C) S_N(\vec{b}_N)) \right|^2 \right\}. \tag{3}$$

We restrict our calculations to a zero-range NN interaction in order to reduce the amount of space integrals since we observe that the interaction range has a small impact on the final nucleon-removal cross section for the cases we studied in this work. In the case of the free (density-independent) NN interaction cross section, Eq. (2) reduces to the usual formulation. The S_C matrix for the core-target system is computed through the full four-dimensional integral of Eq. (2), considering the various density dependences of the in-medium NN interaction cross sections. The imaginary-to-real part ratio of the interaction cross section, dependent on the incident energy, is taken from Ref. [31]. For a ^{9}Be target, a density derived from quantum Monte Carlo calculations based on the AV18 potential is considered [32] but our conclusions do not vary if we consider a Gaussian matter density with a root mean square of 2.36 fm. For reactions on a ^{12}C target, we use a Gaussian matter density with a root mean square of 2.32 fm. The core density is obtained from a Skyrme-EDF calculation with the Sly4 zero-range effective interaction [33] using the HFBRAD code [34]. The removed-nucleon wave function is calculated in a Woods-Saxon potential whose depth and radius are fixed to reproduce the experimental separation energy of the nucleon and mean-square radius of the corresponding HF wave function. A similar equation to Eq. (2) is used for the nucleon S matrix, exchanging the target density ρ_T with the single-particle presence probability of the removed nucleon. The S matrices give also access to reaction and elastic-scattering cross sections.

The calculation of the multidimensional integrals to calculate the phase shifts χ of Eq. (2) has been computed in a four-dimensional box of 20 fm^4. These integrals have been discretized on a regular mesh with a $\delta x = 0.2$ fm integration step. The influence of the step size on the reaction and one-nucleon removal cross sections has been studied and showed, for the studied cases, to be converged for $\delta x = 0.4$ fm with a precision smaller than 1%. The numerical calculation of the spatial integrals have been parallelized in order to be performed in a reasonable time.

We first considered the free NN cross section from Ref. [35] in order to determine the single-particle cross sections for one-nucleon removal from ^{32}Ar, ^{28}S, ^{24}Si, ^{46}Ar, and ^{12}C and compared to corresponding published theoretical results [6,8,13,36]. Our calculation agrees with the latter with a mean deviation of 2% and no systematic trend is observed. Discrepancies can be imputed to the differences of the considered mean-field densities and numerical uncertainties in the integral evaluations.

B. In-medium *NN* cross sections

In-medium NN interaction cross sections constitute one of the basic ingredients in the calculation of the nucleon-removal cross sections. In the present work, we have considered three different sets of in-medium NN interaction cross sections: (i) a set based on a microscopic nonrelativistic Brueckner-Hartree-Fock (BHF) calculation of isospin asymmetric nuclear matter performed by us [22] that uses the realistic Argonne V18 nucleon-nucleon interaction [37] as an input in the Bethe-Goldstone equation, (ii) a cross-section parametrization based on the relativistic Dirac-Brueckner approach of Li and Machleidt (L&M) [24,25] that uses the Bonn nucleon-nucleon potential [38] as bare interaction, and (iii) a phenomenological formula for in-medium NN cross sections developed by Xiangzhou *et al.* (CX) [29]. The Coulomb force is neglected in the three sets of calculations. We present in the following a short review of our calculation and provide a few details about the other two.

The scattering amplitude of two nucleons in the presence of a surrounding nuclear environment is given, in the context of Brueckner theory, by the Brueckner reaction matrix G which

is obtained by solving the Bethe-Goldstone equation

$$G_{\tau_1\tau_2;\tau_3\tau_4}(\omega) = V_{\tau_1\tau_2;\tau_3\tau_4} + \sum_{ij} V_{\tau_1\tau_2;\tau_i\tau_j} \times \frac{Q_{\tau_i\tau_j}}{\omega - \epsilon_{\tau_i} - \epsilon_{\tau_j} + i\eta} G_{\tau_i\tau_j;\tau_3\tau_4}(\omega), \quad (4)$$

where $\tau = n, p$ indicates the isospin projection and the linear momentum of a nucleon in the initial, intermediate, and final state, whereas V denotes the bare NN interaction, in our case the Argonne V18 potential, and $Q_{\tau_i\tau_j}$ the Pauli operator that allows only intermediate states compatible with the Pauli principle. ω designates the so-called starting energy that corresponds to the sum of nonrelativistic energies of the scattered nucleons. The single-particle energy ϵ_τ of a nucleon with momentum $\vec{k}$ is given by

$$\epsilon_\tau(\vec{k}) = \frac{\hbar^2 k^2}{2m_\tau} + \mathrm{Re}[U_\tau(\vec{k})], \quad (5)$$

where the single-particle potential $U_\tau(\vec{k})$ represents the mean field "felt" by a nucleon due to its interaction with the other nucleons of the medium. In the BHF approximation, $U(\vec{k})$ is calculated through the "on-shell energy" G-matrix, and is given by

$$U_\tau(\vec{k}) = \sum_{\tau'} \sum_{|\vec{k}'|<k_{F_{\tau'}}} \langle \vec{k}\vec{k}' \mid G_{\tau\tau';\tau\tau'}(\epsilon_\tau(k) + \epsilon_{\tau'}(k')) \mid \vec{k}\vec{k}' \rangle_A, \quad (6)$$

where the sum runs over all neutron and proton occupied states and where the matrix elements are properly antisymmetrized. It is worth mentioning that in the case of two reacting nuclei such as considered here, the relative velocity of the target and projectile matter densities is not considered in the microscopic determination of Pauli-blocked states. Note that Eqs. (4) and (6) are coupled due to the occurrence of $U_\tau(\vec{k})$ in Eq. (5) and, therefore, they have to be solved self-consistently. Once self-consistency is achieved, the total in-medium NN cross section can be obtained from the G matrix as

$$\sigma_{\tau\tau'} = \frac{m^*_\tau m^*_{\tau'}}{16\pi^2\hbar^4} \sum_{LL'SJ} \frac{2J+1}{4\pi} \left| G^{LL'SJ}_{\tau\tau';\tau\tau'} \right|^2, \quad (7)$$

where $G^{LL'SJ}_{\tau\tau';\tau\tau'}$ is the partial-wave projection of the on-shell G matrix evaluated at the collision energy of the interacting nucleons in the laboratory frame.

It is clear from Eqs. (4) and (6) that medium effects on the NN cross sections arise from Pauli-blocking and from the dispersive effect of the single-particle potential. In our BHF calculation, however, we have considered only medium effects associated with Pauli-blocking in order to make the analysis of the results simpler. We have solved the Bethe-Goldstone equation taking into account only kinetic energies in the particle-particle propagator, and the effective masses appearing in Eq. (7) have been taken equal to the bare nucleon mass. It is expected that the use of the effective masses will lower the in-medium NN cross sections in comparison to the free case and in addition to the reduction induced by Pauli-blocking. However, evaluating the effect of the single-particle potential is not so obvious, since, due to its momentum dependence [see Eq. (6)] and the energy dependence of the G matrix [see Eq. (4)], it can induce either an increase or a decrease of the in-medium NN cross sections compared to the free case. As this effect is not straightforward, it requires a more careful analysis that will be addressed in a future work.

The second considered calculation, quoted as L&M in this paper, uses the Bonn potential in a relativistic Dirac-Brueckner calculation for symmetric nuclear matter in which the effective nucleon scalar and vector fields are obtained in a self-consistent way together with the so-called $\tilde{G}$ matrix by solving the in-medium Thompson equation (relativistic Bethe-Goldstone equation). The in-medium NN cross sections are then calculated in terms of the partial-wave $\tilde{G}$ matrix elements and, finally, fitted by a semi-empirical formula that includes the dependence on the incident energy (ranging from 50 to 300 MeV) and on the total density of nuclear matter (up to 2–$3\rho_0$).

The third considered calculation (CX) uses a phenomenological formula for the in-medium NN interaction cross sections which combines the energy dependence (from 10 MeV to 1 GeV) of the free-space NN interaction cross section of Charagi and Gupta (C&G) [35] with the L&M parametrizations.

Finally, we note here that the in-medium NN cross sections based on our BHF calculation depend also on the isospin asymmetry (i.e., different neutron and proton densities), whereas the other two sets do not include such a dependence. In Fig. 1 we show for comparison the results for the in-medium neutron-proton cross section obtained from the three sets of calculations in function of the incident energy. The full lines show the free-space results, whereas the dashed ones correspond to a density of $\rho = 0.1$ fm^{-3}. From 10 MeV to 300 MeV, our calculations and the CX parametrization are in good agreement with the experimental data. In this region, the L&M parametrization is, in comparison, quite far from the experimental points. At higher energies the CX parametrization, that is obtained from a fit on experimental data up to 1 GeV, sticks to the data whereas our calculation shows a disagreement which increases with energy. This disagreement is expected since our calculation is based on the AV18 potential derived from nucleon-nucleon experimental scattering data up to 300 MeV. The DD effect on the NN-interaction cross section is also very different from one prescription to another. The L&M parametrization shows a 50% reduction of σ_{np} from $\rho = 0$ fm^{-3} to $\rho = 0.1$ fm^{-3}, whereas the DD effect is more moderate for the two other prescriptions. In our work, σ_{np} does not depend significantly on the density above 300 MeV meaning that there are no Pauli-blocked states at these energies in our calculation. On the contrary the CX parametrization shows a constant reduction of about 20% from $\rho = 0$ fm^{-3} to $\rho = 0.1$ fm^{-3} over the whole energy range from 10 MeV to 1 GeV.

III. RESULTS

To illustrate generic trends due to the introduction of density-dependent NN cross sections, we first detail the

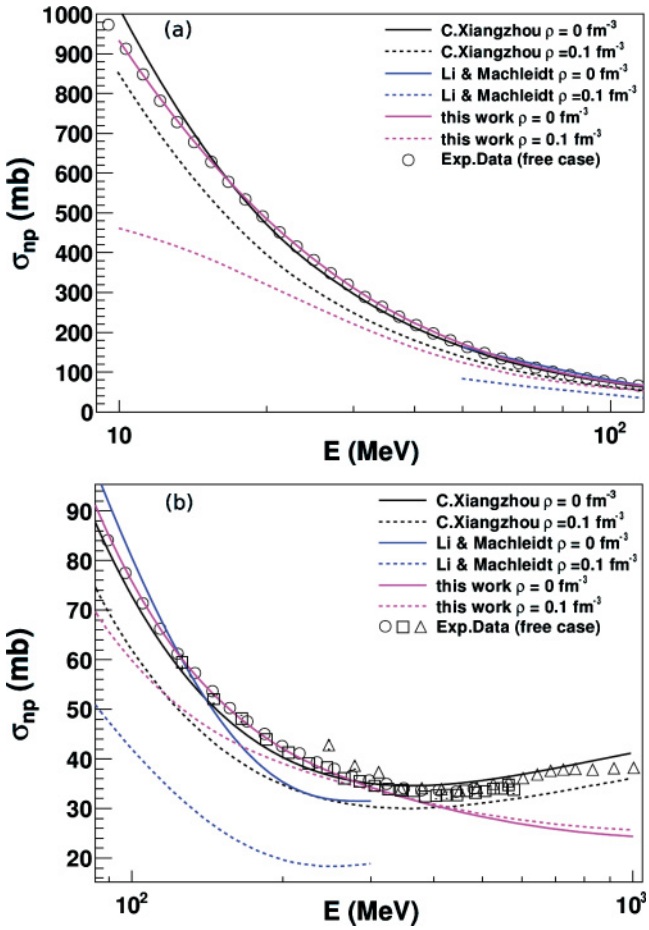

FIG. 1. (Color online) Neutron-proton cross sections obtained from our BHF calculation [22] and the parametrizations of Li and Machleidt [24,25] and of Xiangzhou *et al.* [29]. (Top panel) From 10 to 100 MeV. (Bottom panel) From 100 to 1000 MeV. Experimental data are taken from [39–41].

specific case of the one-neutron removal from ^{24}Si on a ^{9}Be target. Nevertheless similar conclusions have been obtained for other *sd*-shell nuclei, for both proton and neutron knockout, and are presented at the end of this section.

^{24}Si has the particularity to be at the proton dripline. The proton separation energy is $S_p = 3.304$ MeV, whereas neutrons are well bound with a separation energy of $S_n = 21.09$ MeV. The variation with energy of the reaction cross section σ_r is shown in panel (a) of Fig. 2. All parametrizations, with the exception of the one of L&M, are within a few percents of the reaction cross sections calculated with the free NN interaction of C&G [35] over the whole considered energy range. The dominant part of the reactions occurs at the nuclear surface where the density effects are negligible. Such a small impact on σ_r is consistent with the conclusions of Ref. [28].

Single-particle one-neutron removal cross sections have been calculated for a $d_{5/2}$ neutron with a separation energy S_n corresponding to the last filled orbital. For all considered NN interaction cross sections the calculated one-nucleon knockout cross sections increase with energy up to ∼250 MeV/nucleon and remain almost constant beyond [see panel (b) of

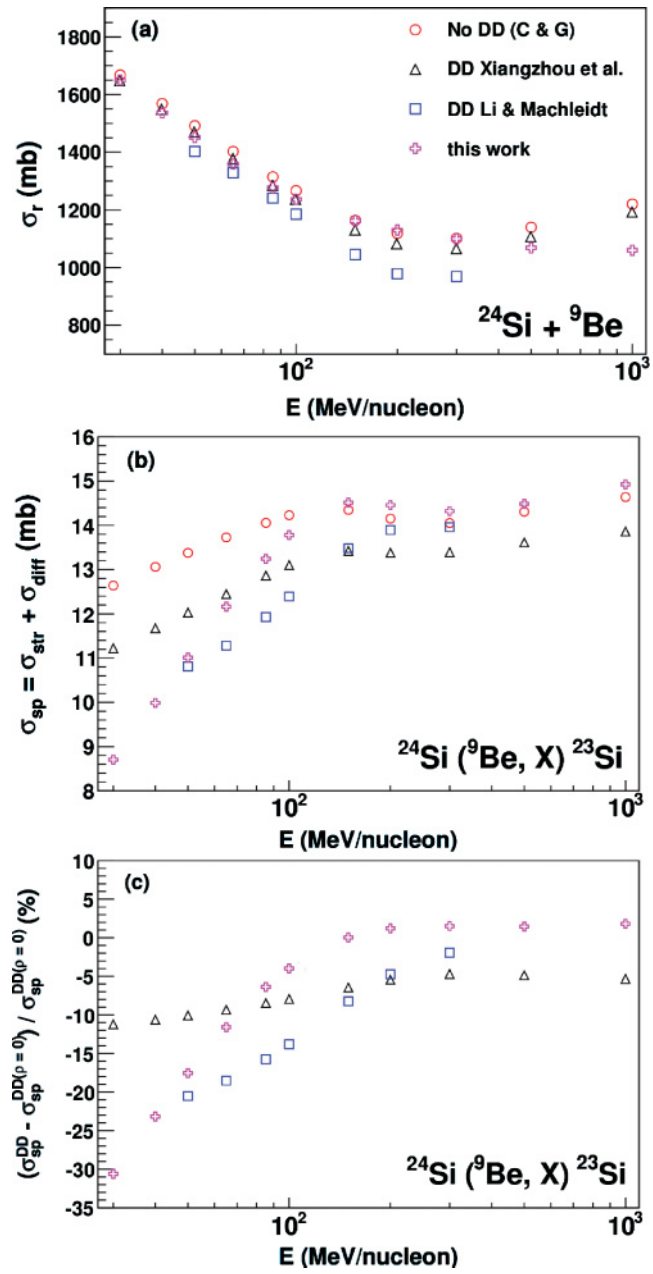

FIG. 2. (Color online) (Top) Reaction cross section of ^{24}Si + ^{9}Be for different energies ranging from 30 MeV/nucleon to 1 GeV/nucleon. (Middle) One-neutron removal cross section ^{24}Si(^{9}Be,X)^{23}Al as a function of incident energy. (Bottom) Effect of the density dependence of the in-medium NN interaction (in %) as a function of incident energy. Three different density-dependent NN interaction cross section calculations are compared (see text).

Fig. 2], due to the slow increase of σ_{NN} with energy beyond the two-pion production threshold. At high energy, calculations based on L&M and our BHF approach reach asymptotically the free NN interaction case, as expected. On the other hand, the calculations based on the CX parametrization do not converge to the free NN interaction case and it seems to be linked to a limit of the parametrization which does not converge to the predictions at $\rho = 0$ for high incident

energies, as previously mentioned. The largest differences are observed at lower energies, below 200 MeV/nucleon. All density-dependent calculations give cross sections below the free-interaction prediction. For example, at 85 MeV/nucleon, the free calculation is 14.0 mb whereas DD predictions are 11.9, 12.9, 13.2 mb for L&M, CX, and our BHF approach, respectively. These differences between free and density-dependent interaction predictions do not only come from the density dependence but also from the initial differences between the considered NN interaction cross sections at zero density. In order to really pinpoint the effect of the density dependence, we compared the variations of the one-nucleon knockout cross sections, for each considered NN interaction, with its full density dependence and without, i.e., with the NN interaction cross section taken at $\rho = 0$ [see panel (c) of Fig. 2]. In all cases, the density dependence lowers the knockout cross section but the DD effect becomes negligible at incident energies above 300 MeV/nucleon. Again, in the case of the CX parametrization, the DD effect does not vanish at large energies because of the parametrization itself. In the case of our BHF calculations, a good asymptotical behavior is observed, thus we only focus on this prescription in the following.

In order to illustrate the effect of Pauli-blocking medium effects that one should expect on typical intermediate-energy knockout experiment results, we performed similar calculations for several other nuclei within or close to the sd shell, considering the knockout of nucleons from orbitals with different ℓ values (s, d, or f). We restrict ourselves to systems studied at intermediate energies at the NSCL and GANIL in order to evaluate the average impact of such density effects on existing data. We gather in Table I our one-nucleon knockout estimates with and without DD for a set of reactions. The same conclusions as for ^{24}Si can be drawn. At energies ranging from 55 to ∼90 MeV/nucleon, the DD effect on one-nucleon knockout cross sections start from 6% to 21%. The studied cases cover a large range of asymmetry,[1] from the removal of very weakly bound to very well bound nucleons. No systematic trend with asymmetry is observed.

TABLE I. Summary of the results for one-proton and one neutron knockout calculations with $\sigma_{NN}(E, \rho)$ based on our BHF approach [22]. Given are the projectile type, its incident energy, the ℓ of the removed nucleon, the single-particle cross sections calculated with $\sigma_{NN}(E, \rho)$, and with $\sigma_{NN}(E, \rho = 0)$ and the difference between both.

Projectile	Target	E (MeV/nucleon)	$n\ell j$	σ_{sp} (mb)	σ_{sp} ($\rho = 0$) (mb)	δ (%)
		Neutron knockout				
^{24}Si	^{9}Be	85.3	$1d_{5/2}$	13.2	14.1	6.4
^{32}Ar	^{9}Be	65.1	$1d_{5/2}$	8.4	9.5	11.2
^{46}Ar	^{9}Be	70.0	$1f_{7/2}$	11.1	12.5	11.3
^{26}Ne	^{9}Be	83.0	$2s_{1/2}$	24.9	28.4	12.3
^{16}C	^{12}C	55.0	$1d_{5/2}$	30.8	38.8	20.6
^{20}O	^{12}C	62.0	$1d_{5/2}$	18.9	23.2	18.5
		Proton knockout				
^{24}Si	^{9}Be	85.3	$1d_{5/2}$	21.1	23.3	9.6

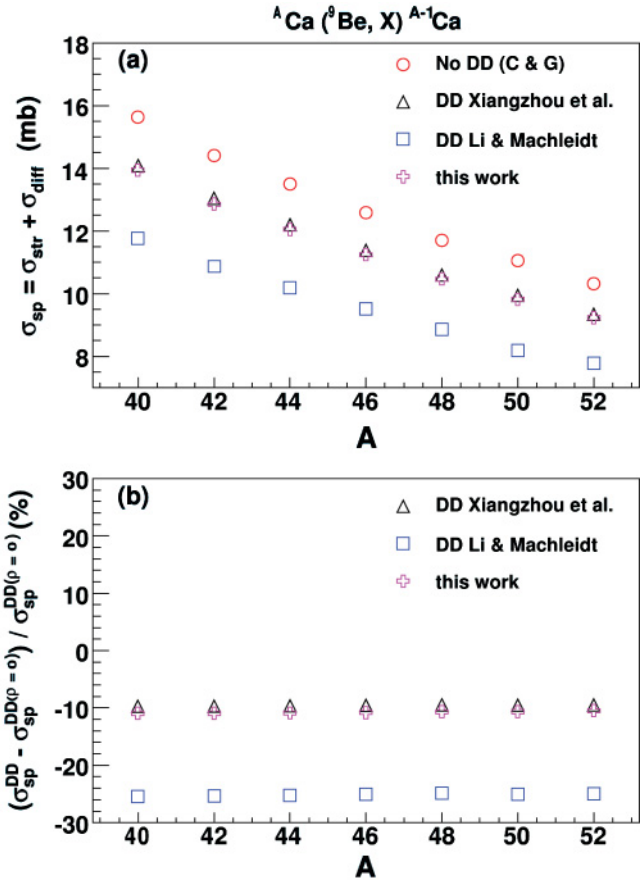

FIG. 3. (Color online) Evolution of the proton knockout cross sections at 80 MeV/nucleon along the calcium isotopic chain for the different parametrizations of σ_{NN}.

Indeed, one may wonder how the density dependence varies, at a given incident energy, for systems with different asymmetry. From a naive point of view, one could expect the effect of the DD to be larger for deeply-bound nucleon removal in exotic nuclei, i.e., from a wave function inside the core density. Single-particle removal cross sections for $d_{3/2}$ protons in calcium isotopes ranging from $A = 40$ to $A = 52$ at 80 MeV/nucleon are shown in Fig. 3 for all previously considered NN interaction cross sections. As expected, the one-nucleon removal cross section decreases with the mass of the isotopes since the $\pi d_{3/2}$ wave function is more and more embedded inside the bulk of the nucleus. The DD effect is shown in the bottom panel of Fig. 3 and has a mean effect of 10% except for the L&M parametrization (25%) as in the case of ^{24}Si [see Fig. 2 panel (c)]. Nevertheless, all DD calculations lead to the same conclusion: the reduction of the one-proton knockout due to Pauli-blocking does not vary over a mass range covering a 12-neutron difference. We therefore conclude that

[1] In this context, we define the asymmetry of a nucleus by the difference of its neutron and proton separation energies as in Ref. [13].

this effect does not play a role in the reduction trend mentioned by Gade *et al.* [8].

IV. CONCLUSIONS

We have performed calculations of single-particle cross sections for one-nucleon removal reactions at intermediate energies using in-medium NN cross sections based on a BHF calculation of isospin asymmetric nuclear matter [22], and on two different parametrizations from L&M [24,25] and CX [29]. The nucleon-removal calculations have been performed within the S-matrix formalism under the Glauber approximation. In our BHF approach, we have taken into account only kinetic energies when solving the Bethe-Goldstone equation as well as bare nucleon masses in order to consider only medium effects in the NN cross sections associated with Pauli-blocking. The relative velocity of the two interacting nuclei is not included in the determination of the Pauli-blocked states when the NN interaction cross section is derived. The effect of the single-particle potential, the effective masses and the effect of the relative velocity between target and projectile matter densities on the Pauli-blocked state distribution should be addressed in a future work. Results obtained with our BHF approach show the right asymptotic behavior at high incident energy, which validates this approach for forthcoming calculations. We have observed that in general the inclusion of a realistic density-dependence in the NN interaction decreases the single-particle cross section up to 20% for incident energies higher than 50 MeV/nucleon, which is of the same order as the variation brought by other sources of uncertainty. These effects are predicted to be reduced to less than a few percents at higher incident energies $\geqslant$200 MeV/nucleon. The present formalism allows to estimate the Pauli-Blocking medium effects in the extraction of absolute spectroscopic factors from one-nucleon removal experiments at intermediate energies.

ACKNOWLEDGMENTS

This work has been partially supported by FEDER/FCT (Portugal) under the project CERN/FP/83505/2008. One of the authors (I.V.) thanks Arthur Polls and Angels Ramos for useful and stimulating discussions.

[1] M. Baranger, Nucl. Phys. **A149**, 225 (1970).
[2] G. Jacob and Th. A. J. Maris, Rev. Mod. Phys. **38**, 121 (1966).
[3] G. Ray Satchler, Rev. Mod. Phys. **50**, 1 (1978).
[4] R. J. Glauber, in *Lecture Notes in Theoretical Physics*, edited by W. E. Britten and L. G. Dunham (Interscience, New York, 1958), vol. 1, pp. 315–414.
[5] G. J. Kramer, H. P. Blok, and L. Lapikás, Nucl. Phys. **A679**, 267 (2001).
[6] B. A. Brown, P. G. Hansen, B. M. Sherrill, and J. A. Tostevin, Phys. Rev. C **65**, 061601(R) (2002).
[7] J. Lee, J. A. Tostevin, B. A. Brown, F. Delaunay, W. G. Lynch, M. J. Saelim, and M. B. Tsang, Phys. Rev. C **73**, 044608 (2006).
[8] A. Gade *et al.*, Phys. Rev. Lett. **93**, 042501 (2004).
[9] P. G. Hansen and J. A. Tostevin, Annu. Rev. Nucl. Part. Sci. **53**, 219 (2003).
[10] J. A. Tostevin, J. Phys. G: Nucl. part. Phys. **25**, 735 (1999).
[11] F. Carstoiu, E. Sauvan, N. A. Orr, and A. Bonaccorso, Phys. Rev. C **70**, 054602 (2004).
[12] A. Bonaccorso and F. Carstoiu, Phys. Rev. C **61**, 034605 (2000).
[13] A. Gade *et al.*, Phys. Rev. C **77**, 044306 (2008).
[14] P. Batham, I. J. Thompson, and J. A. Tostevin, Phys. Rev. C **71**, 064608 (2005).
[15] A. Sakharuk and V. Zelevinsky, Phys. Rev. C **61**, 014609 (1999).
[16] A. Bohnet, N. Ohtsuka, J. Achelin, R. Linden, and A. Faessler, Nucl. Phys. **A494**, 349 (1989).
[17] T. Alm, G. Röpke, and M. Schmidt, Phys. Rev. C **50**, 31 (1994).
[18] G. Giansiracusa, U. Lombardo, and N. Sandulescu, Phys. Rev. C **53**, R1478 (1996).
[19] H.-J. Schulze, A. Schnell, G. Röpke, and U. Lombardo, Phys. Rev. C **55**, 3006 (1997).
[20] A. Schnell, G. Röpke, U. Lombardo, and H.-J. Schulze, Phys. Rev. C **57**, 806 (1998).
[21] H. F. Zhang, Z. H. Li, U. Lombardo, P. Y. Luo, F. Sammarruca, and W. Zuo, Phys. Rev. C **76**, 054001 (2007).
[22] I. Vidaña (in preparation, 2009).
[23] B. ter Haar and R. Malfliet, Phys. Rep. **149**, 207 (1987); Phys. Rev. C **36**, 1611 (1987).
[24] G. Q. Li and R. Machleidt, Phys. Rev. C **48**, 1702 (1993).
[25] G. Q. Li and R. Machleidt, Phys. Rev. C **49**, 566 (1994).
[26] C. Fuchs, A. Faessler, and M. El-Shabshiry, Phys. Rev. C **64**, 024003 (2001).
[27] V. R. Pandharipande and S. C. Pieper, Phys. Rev. C **45**, 791 (1992).
[28] R. E. Warner, I. J. Thompson, and J. A. Tostevin, Phys. Rev. C **65**, 044617 (2002).
[29] Cai Xiangzhou, Feng Jun, Shen Wenqing, Ma Yuang, Wang Jiansong, and Ye Wei, Phys. Rev. C **58**, 572 (1998).
[30] F. Barranco and E. Vigezzi, in *International School of Heavy-Ion Physics*, 4th course, edited by R. A. Broglia and P. G. Hansen (World Scientific, Singapore, 1998).
[31] L. Ray, Phys. Rev. C **20**, 1857 (1979).
[32] S. C. Pieper, K. Varga, and R. B. Wiringa, Phys. Rev. C **66**, 044310 (2002).
[33] E. Chabanat *et al.*, Nucl. Phys. **A627**, 710 (1997).
[34] K. Bennaceur and J. Dobaczewski, Comput. Phys. Commun. **168**, 96 (2005).
[35] S. K. Charagi and S. K. Gupta, Phys. Rev. C **41**, 1610 (1990).
[36] A. Gade *et al.*, Phys. Rev. C **71**, 051301(R) (2005).
[37] R. B. Wiringa, V. G. J. Stoks, and R. Schiavilla, Phys. Rev. C **51**, 38 (1995).
[38] R. Machleidt, Adv. Nucl. Phys. **19**, 189 (1989).
[39] W. P. Abfalterer, F. B. Bateman, F. S. Dietrich, R. W. Finlay, R. C. Haight, and G. L. Morgan, Phys. Rev. C **63**, 044608 (2001).
[40] V. Grundies *et al.*, Phys. Lett. **B158**, 15 (1985).
[41] T. J. Devlin *et al.*, Phys. Rev. D **8**, 136 (1973).